

Performance Guarantees for Data Freshness in Resource-Constrained Adversarial IoT Systems

Aresh Dadlani*, Muthukrishnan Senthil Kumar†, Omid Ardakanian‡, and Ioanis Nikolaidis‡,

*Department of Mathematics and Computing, Mount Royal University, Calgary, Canada

†Department of Applied Mathematics and Computational Sciences, PSG College of Technology, Coimbatore, India

‡Department of Computing Science, University of Alberta, Edmonton, Canada

Emails: adadlani@mtroyal.ca, msk.amcs@psgtech.ac.in, {ardakanian, nikolaidis}@ualberta.ca

Abstract—Timely updates are critical for real-time monitoring and control applications powered by the Internet of Things (IoT). As these systems scale, they become increasingly vulnerable to adversarial attacks, where malicious agents interfere with legitimate transmissions to reduce data rates, thereby inflating the age of information (AoI). Existing adversarial AoI models often assume stationary channels and overlook queueing dynamics arising from compromised sensing sources operating under resource constraints. Motivated by the G-queue framework, this paper investigates a two-source M/G/1/1 system in which one source is adversarial and disrupts the update process by injecting negative arrivals according to a Poisson process and inducing i.i.d. service slowdowns, bounded in attack rate and duration. Using moment generating functions, we then derive closed-form expressions for average and peak AoI for an arbitrary number of sources. Moreover, we introduce a worst-case constrained attack model and employ stochastic dominance arguments to establish analytical AoI bounds. Numerical results validate the analysis and highlight the impact of resource-limited adversarial interference under general service time distributions.

Index Terms—Age of information, adversarial arrivals, general service time, M/G/1/1 queue, performance bounds

I. INTRODUCTION

The convergence of Internet of Things (IoT) platforms with low-latency 5G connectivity has enabled a new class of real-time applications such as environmental monitoring, industrial automation, and remote healthcare [1]. These systems rely on distributed sensing devices to generate time-stamped status updates for analysis and control at a receiver. In such time-sensitive settings, the *freshness* of received information is critical for maintaining system responsiveness, control stability, and quality of experience. Traditional performance metrics, such as throughput and delay, fail to capture this notion of timeliness from the perspective of the monitor. To address this requirement, the *age of information* (AoI) metric has been introduced to quantify the time elapsed since the most recently received update was generated [2]–[4].

Minimizing AoI in IoT systems is an active research area that requires a nuanced understanding of the dynamics that govern status delivery. To model the inherent delays caused by physical separation, channel contention, and access protocols, the communication link is often represented as a queueing system. Early works studied how contention and scheduling affect AoI in single-source settings under various service disciplines and access strategies [5], and subsequent studies ex-

tended these models to multi-source [6]–[8] and multi-hop [9]–[11] networks with heterogeneous update generation, buffer constraints, and packet management mechanisms.

A growing challenge in large-scale IoT deployments is vulnerability to malicious attacks that exploit protocol properties and flaws to inflate information freshness. Such disruptions are particularly detrimental in real-time applications, where delayed or outdated updates can compromise safety and control performance. Much of the existing literature focuses on optimizing AoI under stationary wireless channel conditions with additive noise, fading, and unintentional interference [12], [13]. However, the stationarity assumption is unsuitable for adversarial settings, where attackers can dynamically disrupt transmissions or degrade link quality. In [14], game-theoretic strategies are developed to characterize equilibrium behavior in adversarially jammed status update systems. While all these efforts ([12]–[14]) provide valuable insights, they do not explicitly examine adversarial interference from a queueing-theoretic perspective. In practice, adversaries are often resource constrained and may be limited by transmission power or spectrum access. For example, an attacker using directional interference to disrupt a communication channel may be unable to consistently track a moving receiver and therefore can only interfere sporadically. The impact of such constrained adversarial (negative) arrivals, modeled within the G-queue framework [15], on AoI remains largely unexplored. A related study modeled negative Poisson arrivals in an M/M/1/1 system that remove all queued updates [16]. Nonetheless, the analysis does not extend to non-Markovian service time distributions or service slowdowns under physical constraints limiting sustained attacks.

This paper analyzes AoI under adversarial interference, modeled as negative arrivals, in a two-source M/G/1/1 system. We first derive closed-form moment generating functions (MGFs) for average AoI (AAoI) and peak AoI (PAoI) under adversarial disruptions consistent with real-world IoT attacker constraints. We then extend the MGF-based approach to generalize the analysis for multi-source M/G/1/1 queues subject to similar adversarial conditions and derive lower and upper bounds on AAoI for the worst-case adversarial model. We assume the attacker cannot continuously interfere with the system due to limited battery, spectrum access restrictions, or the risk of detection. This constraint ensures a physically plausible attack model and allows for meaningful AoI performance guarantees.

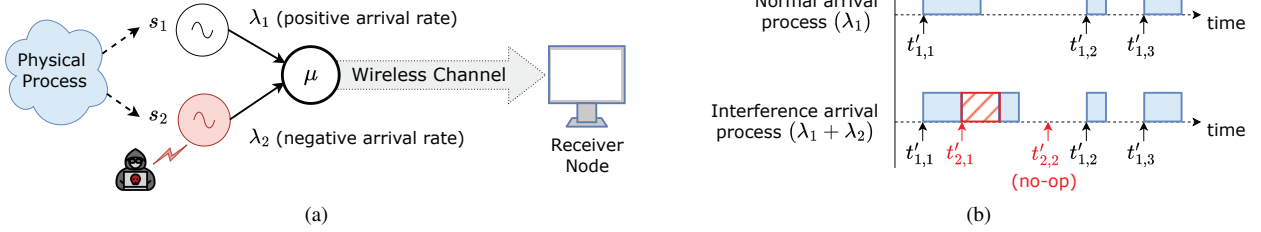


Fig. 1. Schematic of a real-time monitoring system under attack: (a) Two IoT sensing devices with one compromised (s_2). (b) Timeline showing the impact of negative arrivals on the service times of status updates. Idle injections ($t'_{2,2}$) have no effect (no-op), while collisions ($t'_{2,1}$) preempt updates, causing delayed service and increased AoI.

Finally, we present numerical results to validate the theoretical findings and demonstrate the impact of adversarial interference under general service time distributions and independent and identically distributed (i.i.d.) service slowdowns.

II. SYSTEM MODEL AND DEFINITIONS

We consider the real-time IoT monitoring system illustrated in Fig. 1a, where a sensor observes an underlying physical process and generates time-stamped status updates. An adversarial process, acting through a compromised sensor, injects attack traffic into the communication channel. The system is modeled as an M/G/1/1 queue, where updates are served in order of arrival, and at most one update can be accommodated at any time. The service time distribution models the time required for successful reception of an update, and the departure instant from the queue corresponds to its reception at the destination. The benign source transmits informative (positive) status updates according to a Poisson process with rate $\lambda_1 > 0$, while the compromised source generates disruptive (negative) arrivals following an independent Poisson process with rate $\lambda_2 > 0$. Negative arrivals, though carrying no useful information, disturb the channel by preempting any positive packet in service. Such disruptions can arise from actions like jamming, reducing the channel bitrate, or triggering retransmissions, effectively prolonging the update reception time. This setup captures attacks within the G-queue framework, where negative arrivals disrupt the queueing discipline and degrade system performance. To ensure physical plausibility, we bound the adversary's attack rate by $\lambda_2 \leq \lambda_{\max}$. This bounded-threat assumption enables meaningful AoI performance guarantees under realistic adversarial conditions while still allowing for worst-case strategies within the limit.

An illustrative example of this process is depicted in Fig. 1b. Let $t_{i,j}$ denote the generation time of the j -th update from source s_i and $t'_{i,j}$ its reception time at the receiver. Under normal operation, updates generated by source s_1 arrive at time instants $t'_{1,j}$, where $j \in \{1, 2, 3\}$. For the negative arrivals at $t'_{2,j'}$, where $j' \in \{1, 2\}$, idle injections ($t'_{2,2}$) have no effect (no-op), whereas in-service preemptions ($t'_{2,1}$) force retransmissions or re-encoding. These interruptions elongate effective service times by inducing service slowdowns for subsequent update transmissions, increase inter-delivery intervals, and inflate AoI. The normal service time of an update from source s_1 is denoted

by the continuous random variable (r.v.) S_n , with probability density function (pdf) $f_{S_n}(\cdot)$, cumulative distribution function (cdf) $F_{S_n}(t) = \int_0^t f_{S_n}(u) du = \Pr(S_n \leq t)$, and moment generating function (MGF) $M_{S_n}(s) = \mathbb{E}[e^{sS_n}]$. Unlike [16], following a negative arrival, the service time is increased according to the continuous r.v. $S_s = \beta S_n$, characterized by pdf $f_{S_s}(\cdot)$ and MGF $M_{S_s}(s) = \mathbb{E}[e^{sS_s}]$. After an exponentially distributed sojourn in the slow state with mean $1/\Lambda$, where $\Lambda \triangleq \lambda_1 + \lambda_2$, the server resumes normal service. The slowdown factor, $1 < \beta \leq \beta_{\max}$, models the operational limits on the adversary and ensures that the server cannot be forced into a persistently degraded state.

AoI is the time elapsed since the generation of the most recently received update at the destination, making it a fundamental measure of information freshness. At any given time τ , the most recently received update is indexed by $N_i(\tau) \triangleq \max \{j' \mid t'_{i,j'} \leq \tau\}$ [6]. Typically exhibiting a sawtooth pattern, the instantaneous AoI of s_i at time t is defined by the random process $A_i(t) \triangleq t - \psi_i(t)$, where $\psi_i(\tau) = t_{i,N_i(\tau)}$ is the generation time of the latest received update from s_i . Consequently, the AAoI of source s_i over interval $(0, T)$ is:

$$\bar{\Delta}_i = \frac{1}{T} \int_0^T A_i(t) dt. \quad (1)$$

A more mathematically tractable metric is the PAoI, which captures the maximum AoI value immediately before the reception of a new update, and is given as $P_{i,j} = t'_{i,j} - t_{i,j-1}$ [5]. PAoI essentially quantifies the maximum staleness experienced between consecutive successfully delivered updates.

III. AOI AND PAOI IN ADVERSARIAL M/G/1/1 QUEUES

In this section, we analyze the age metrics in an M/G/1/1 queue subject to adversarial arrivals. To facilitate our analysis, we relate AoI with two key random variables associated with the j -th successfully delivered update from source s_i . The *system time* ($T_{i,j}$) is the total time from the generation of an update until its reception at the destination and is calculated as $T_{i,j} = t'_{i,j} - t_{i,j}$. The *inter-departure time* ($Y_{i,j}$) is the time between the reception of the $(j-1)$ -th and the j -th delivered updates, and is given as $Y_{i,j} = t'_{i,j} - t'_{i,j-1}$. Therefore, the PAoI of the j -th update can be expressed as:

$$P_{i,j} = Y_{i,j} + T_{i,j-1}. \quad (2)$$

Assuming the system is stationary and the AoI process is ergodic, we drop the subscript j in derivations that follow. Therefore, for source s_i , we denote the system and inter-departure times by T_i and Y_i , respectively, with MGFs $M_{T_i}(s) \triangleq \mathbb{E}[e^{sT_i}]$ and $M_{Y_i}(s) \triangleq \mathbb{E}[e^{sY_i}]$.

A. Age in the Two-Source Adversarial Model

We consider the two-source case introduced in Section II, where sources s_1 and s_2 generate positive and negative packets, respectively. Let A_i and P_i denote, respectively, the AoI and PAoI of updates from source s_i , where $i \in \{1, 2\}$, with MGFs $M_{A_i}(s) \triangleq \mathbb{E}[e^{sA_i}]$ and $M_{P_i}(s) \triangleq \mathbb{E}[e^{sP_i}]$. Following the general M/G/1/1 AoI characterization in [7], the MGFs of AoI and PAoI for the benign source s_1 are given as:

$$M_{A_1}(s) = \frac{M_{T_1}(s) (M_{Y_1}(s) - 1)}{s M'_{Y_1}(0)}, \quad (3)$$

$$M_{P_1}(s) = M_{T_1}(s) M_{Y_1}(s), \quad (4)$$

where $M'_{Y_1}(0)$ denotes the first derivative of $M_{Y_1}(s)$ at $s = 0$. To obtain closed-form expressions for (3) and (4), we require explicit derivations of $M_{T_1}(s)$ and $M_{Y_1}(s)$.

1) *Derivation of $M_{T_1}(s)$* : With T_1 representing the system time of a *successfully delivered* update from source s_1 , let \mathcal{D} be the event that a positive update completes service before any negative arrival from source s_2 . Therefore, for an infinitesimal $\epsilon > 0$, the distribution of T_1 satisfies [17]:

$$\begin{aligned} \Pr(T_1 \in [t, t + \epsilon)) &= \Pr(S_n \in [t, t + \epsilon) \mid \mathcal{D}) \\ &= \frac{\Pr(S_n \in [t, t + \epsilon)) \Pr(\mathcal{D} \mid S_n \in [t, t + \epsilon))}{\Pr(\mathcal{D})}. \end{aligned} \quad (5)$$

Taking the limit of (5) yields the pdf of T_1 as follows:

$$f_{T_1}(t) = \lim_{\epsilon \rightarrow 0} \frac{\Pr(T_1 \in [t, t + \epsilon))}{\epsilon} = \frac{f_{S_n}(t) \Pr(\mathcal{D} \mid S_n > t)}{\Pr(\mathcal{D})}. \quad (6)$$

Since the event \mathcal{D} occurs only if no negative arrivals occur during the service period of length t , we have:

$$\Pr(\mathcal{D} \mid S_n > t) = e^{-\lambda_2 t}, \quad (7)$$

$$\text{and } \Pr(\mathcal{D}) = \int_0^\infty e^{-\lambda_2 t} f_{S_n}(t) dt = M_{S_n}(-\lambda_2). \quad (8)$$

Therefore, plugging (7) and (8) into (6) results in $f_{T_1}(t) = f_{S_n}(t) e^{-\lambda_2 t} / M_{S_n}(-\lambda_2)$, which directly leads to the following MGF:

$$M_{T_1}(s) = \frac{M_{S_n}(s - \lambda_2)}{M_{S_n}(-\lambda_2)}. \quad (9)$$

2) *Derivation of $M_{Y_1}(s)$* : Departing from the preemptive M/G/1/1 analysis in [7], our derivation of $M_{Y_1}(s)$ accounts for the adversarial impact of negative arrivals on the service time distribution. We model Y_1 , the inter-departure time between two consecutive *delivered* updates from source s_1 , using the semi-Markov chain shown in Fig. 2. Here, q_0 , q_1 , and q_2 denote the possible states of the system. Specifically, q_0 represents the idle

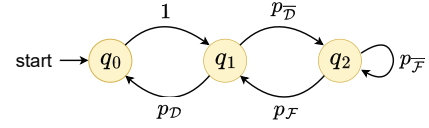


Fig. 2. Semi-Markov chain for the M/G/1/1 inter-departure time Y_1 .

state in which the system awaits the arrival of a fresh positive update, q_1 corresponds to the state where a positive update is being served under normal conditions, and q_2 denotes the state in which, following a preemption event by a negative arrival, the positive update is served at a reduced (slow) service rate. Upon successful delivery of an s_1 update, the system regenerates in state q_0 . These state transitions are formalized as follows:

- $q_0 \rightarrow q_1$: In state q_0 , the system remains idle and awaits the arrival of a positive update. Upon such an arrival, it deterministically transitions to q_1 with probability 1, where the update immediately begins normal service. The sojourn time in q_0 , denoted by W_1 , follows an exponential distribution with rate λ_1 , i.e., $W_1 \sim \text{Exp}(\lambda_1)$.
- $q_1 \rightarrow q_0$: In state q_1 , the system serves the positive update under normal conditions. If the service completes without preemption, the state transitions back to q_0 with probability $p_D \triangleq \Pr(\mathcal{D}) = M_{S_n}(-\lambda_2)$. The sojourn time in q_1 prior to this transition, denoted W_2 , has the same distribution as the system time T_1 conditioned on successful delivery, i.e., $\Pr(W_2 > t) = \Pr(S_n > t \mid \mathcal{D})$.
- $q_1 \rightarrow q_2$: If there is a negative arrival while a positive update is in normal service, the service is preempted, and the system transitions from q_1 to q_2 with probability $p_{\bar{D}} \triangleq 1 - \Pr(\mathcal{D}) = 1 - M_{S_n}(-\lambda_2)$. The sojourn time of the system in q_1 preceding this transition, denoted by W_3 , is distributed as T_1 conditioned on negative preemption, i.e., $\Pr(W_3 > t) = \Pr(S_n > t \mid \bar{\mathcal{D}})$.
- $q_2 \rightarrow q_1$: If the slowdown period ends before the update in q_2 completes service, the system switches back to q_1 , resuming normal service. Let \mathcal{F} denote the event that the service completes before a negative arrival from source s_2 , and $\bar{\mathcal{F}}$ its complement. The probability of completion is given as $p_F \triangleq \Pr(\mathcal{F}) = M_{S_s}(-\Lambda)$. The sojourn time in q_2 before this transition, denoted W_4 , is given as $\Pr(W_4 > t) = \Pr(S_s > t \mid \mathcal{F})$.
- $q_2 \rightarrow q_2$: When in state q_2 , the system serves a positive update at the slow rate. This transition from state q_2 to itself corresponds to event $\bar{\mathcal{F}}$, i.e., a new negative arrival before service completion, which causes the slow service to be preempted and restarted with probability $p_{\bar{F}} \triangleq 1 - \Pr(\mathcal{F}) = 1 - M_{S_s}(-\Lambda)$. The sojourn time in q_2 prior to this transition, denoted as W_5 , is determined similar to W_3 (i.e., the $q_1 \rightarrow q_2$ transition), and is detailed in Lemma 1 below.

Lemma 1. *The pdf of the random variable W_3 is given by:*

$$f_{W_3}(t) = \frac{(1 - F_{S_n}(t)) \lambda_2 e^{-\lambda_2 t}}{1 - M_{S_n}(-\lambda_2)}. \quad (10)$$

Proof. The random variable W_3 is the sojourn time in state

q_1 prior to a preemption by a negative arrival, and thus has the same distribution as the system time T_1 under preemption. Let $H_2 \sim \text{Exp}(\lambda_2)$ denote the inter-arrival time of adversarial packets, and let $\overline{\mathcal{D}}$ denote the event of a negative arrival before normal service completes. Conditioning on $\overline{\mathcal{D}}$, we get:

$$\begin{aligned} f_{W_3}(t) &= \lim_{\epsilon \rightarrow 0} \frac{\Pr(H_2 \in [t, t + \epsilon) \mid \overline{\mathcal{D}})}{\epsilon} \\ &= \lim_{\epsilon \rightarrow 0} \frac{\Pr(H_2 \in [t, t + \epsilon)) \Pr(\overline{\mathcal{D}} \mid H_2 \in [t, t + \epsilon))}{\Pr(\overline{\mathcal{D}}) \epsilon} \\ &= \frac{\Pr(S_n > t) f_{H_2}(t)}{\Pr(\overline{\mathcal{D}})} = \frac{(1 - F_{S_n}(t)) \lambda_2 e^{-\lambda_2 t}}{1 - M_{S_n}(-\lambda_2)}, \end{aligned}$$

where $\Pr(\overline{\mathcal{D}}) = 1 - M_{S_n}(-\lambda_2)$ follows from evaluating the Laplace-Stieltjes transform (LST) of S_n at λ_2 . \square

The inter-departure time between two consecutively delivered updates from source s_1 equals the total sojourn accumulated by the system as it regenerates from state q_0 back to q_0 . This total sojourn time is the sum of the individual sojourns associated with each state and transitions along all paths of the form $\{q_0, \dots, q_0\}$. Consequently, Y_1 can be expressed as:

$$Y_1 = W_1 + W_2 + W_3 + mW_4 + W_5, \quad (11)$$

where $m \geq 0$ counts the number of occurrences of W_4 during the cycle from q_0 to q_0 . For example, one possible realization of this cycle is:

$$\{q_0 \rightarrow q_1, q_1 \rightarrow q_2, q_2 \rightarrow q_2, q_2 \rightarrow q_2, q_2 \rightarrow q_1, q_1 \rightarrow q_0\},$$

which occurs with probability $p_{\mathcal{F}} p_{\mathcal{D}} (1 - p_{\mathcal{D}}) (1 - p_{\mathcal{F}})^2$. Following the methodology in [7], the MGF of Y_1 in (11) is thus calculated as:

$$\begin{aligned} M_{Y_1}(s) &= \mathbb{E}[e^{sY_1}] = \mathbb{E}[e^{s(W_1 + W_2 + W_3 + mW_4 + W_5)}] \\ &= \sum_{m=0}^{\infty} p_{\mathcal{D}} p_{\mathcal{F}} (1 - p_{\mathcal{D}}) (1 - p_{\mathcal{F}})^m \mathbb{E}[e^{s(W_1 + W_2 + W_3 + mW_4 + W_5)}], \end{aligned} \quad (12)$$

where the MGFs of the individual sojourn times are given by:

$$\mathbb{E}[e^{sW_1}] = \frac{\lambda_1}{\lambda_1 - s}, \quad (13)$$

$$\mathbb{E}[e^{sW_2}] = \frac{M_{S_n}(s - \lambda_2)}{M_{S_n}(-\lambda_2)}, \quad (14)$$

$$\mathbb{E}[e^{sW_3}] = \frac{\lambda_2 (1 - M_{S_n}(s - \lambda_2))}{(s - \lambda_2) (M_{S_n}(-\lambda_2) - 1)}, \quad (15)$$

$$\mathbb{E}[e^{sW_4}] = \frac{M_{S_s}(s - \Lambda)}{M_{S_s}(-\Lambda)}, \quad (16)$$

$$\mathbb{E}[e^{sW_5}] = \frac{\Lambda (1 - M_{S_s}(s - \Lambda))}{(s - \Lambda) (M_{S_s}(-\Lambda) - 1)}. \quad (17)$$

Finally, substituting (9) and (12) into (3) and (4) yields closed-form expressions for the MGFs of the AoI and PAoI for source s_1 .

Remark 1. The n^{th} -order moment of the AoI (or PAoI) of source s_1 can be obtained by evaluating the n^{th} derivative of its MGF at $s = 0$. In particular, the first derivative yields the average AoI, $\bar{\Delta}_1$ (or average PAoI, \bar{P}_1):

$$\bar{\Delta}_1 = \left. \frac{dM_{A_1}(s)}{ds} \right|_{s=0}, \quad \bar{P}_1 = \left. \frac{dM_{P_1}(s)}{ds} \right|_{s=0}. \quad (18)$$

B. Extension to the Multi-Source Adversarial Model

The MGF-based framework developed in the preceding subsection can be directly extended to the case of N sources. Let source s_c generate adversarial packets at rate λ_c , and λ_i denote the arrival rate of positive updates from source s_i ($i \neq c$). The aggregate arrival rate of all packets is $\Lambda = \sum_{k=1}^N \lambda_k$. By applying Lemma 1, the pdf and MGF of the system time T_i for an update from source s_i are:

$$f_{T_i}(t) = \frac{f_{S_n}(t) \lambda_c e^{-\lambda_c t}}{M_{S_n}(-\lambda_c)}, \quad M_{T_i}(s) = \frac{M_{S_n}(s - \lambda_c)}{M_{S_n}(-\lambda_c)}. \quad (19)$$

Following the same reasoning as in the two-source case, the MGFs of the AoI and PAoI for source s_i are given as:

$$M_{A_i}(s) = \frac{M_{S_n}(s - \lambda_c) (M_{Y_i}(s) - 1)}{s M_{S_n}(-\lambda_c) M_{Y_i}(0)}, \quad (20)$$

$$M_{P_i}(s) = \frac{M_{S_n}(s - \lambda_c) M_{Y_i}(s)}{M_{S_n}(-\lambda_c)}, \quad (21)$$

where $M_{Y_i}(s)$ is the MGF of the inter-departure time for s_i from state q_0 back to q_0 , obtained by replacing the parameters λ_1 and λ_2 in (13)-(17) with λ_i and λ_c , respectively.

IV. PERFORMANCE BOUNDS OF AAoI

Let H_i denote the inter-arrival time between two consecutive updates from the benign source s_i , $i \in \{1, 2, \dots, N\}$, and let H_c be the inter-arrival time of adversarial arrivals from the compromised source s_c ($i \neq c$). From the renewal reward framework, the time average AoI for source s_i is given by [18]:

$$\bar{\Delta}_i = \mathbb{E}[T_i] + \frac{\mathbb{E}[(Y_i)^2]}{2 \mathbb{E}[Y_i]}. \quad (22)$$

Because the system has no buffer and is subject to preemption by negative arrivals, an update generated by source s_i may be dropped or delayed, which can only increase the time between consecutive *delivered* updates. Hence, $Y_i \geq H_i$, which implies that $\mathbb{E}[Y_i] \geq \mathbb{E}[H_i]$ and $\mathbb{E}[(Y_i)^2] \geq \mathbb{E}[(H_i)^2]$. As a result of this, the following immediate policy-independent *lower bound* on AAoI holds:

$$\bar{\Delta}_i \geq \mathbb{E}[T_i] + \frac{\mathbb{E}[(H_i)^2]}{2 \mathbb{E}[H_i]}. \quad (23)$$

To formulate the worst-case attack model, we consider the adversary s_c to be limited by: (i) the attack rate limit ($\lambda_c \leq \lambda_{\max}$) and the service slowdown factor ($1 < \beta \leq \beta_{\max}$). These constraints reflect practical limitations that prevent the attacker from indefinitely attacking or excessively slowing the server. Let $\mathcal{L}(\lambda_{\max}, \beta_{\max})$ be the set of all admissible attack policies

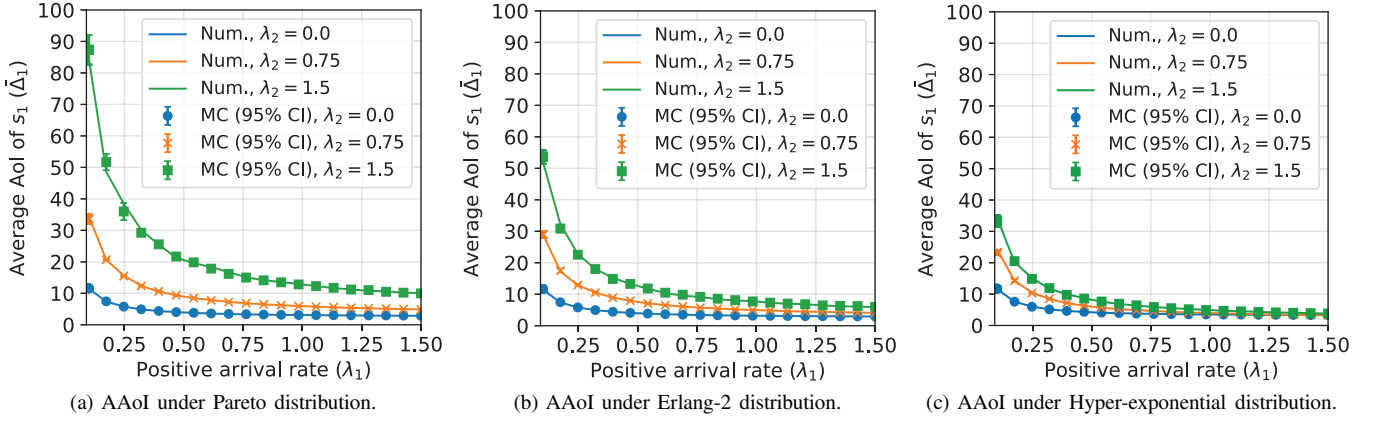


Fig. 3. AAOI comparison in the two-source M/G/1/1 system with adversarial source s_2 under different service distributions and negative arrival rates $\lambda_2 \in \{0, 0.75, 1.5\}$: (a) Pareto ($\theta = 1, \alpha = 3$); (b) Erlang-2 ($k = 2, \mu = 4/3$); (c) Hyper-exponential ($p = 0.5, \mu_1 = 1, \mu_2 = 0.5$). Here, $\beta = 1.5$.

satisfying these constraints. Lemma 2 postulates the worst-case AAOI *upper bound*.

Lemma 2. *For any attack policy $L \in \mathcal{L}(\lambda_{\max}, \beta_{\max})$ and any benign source s_i , where $i \in \{1, 2, \dots, N\}$ and $i \neq c$, the age process $A_i(t)$ is stochastically dominated (in the increasing-convex order) by that under the worst-case policy \mathcal{P}^* that uses $\lambda_c = \lambda_{\max}$ and $\beta = \beta_{\max}$. Consequently, $\forall i \neq c$,*

$$\bar{\Delta}_i \leq \bar{\Delta}_i^{\mathcal{P}^*} = \mathbb{E}[T_i] + \frac{\mathbb{E}[(Y_i^{\mathcal{P}^*})^2]}{2\mathbb{E}[Y_i^{\mathcal{P}^*}]}, \quad (24)$$

where $Y_i^{\mathcal{P}^*}$ includes the slow-service effect and its moments are obtained from the MGFs derived in Section III-B by substituting $\lambda_c = \lambda_{\max}$ and $M_{S_s}(s) = M_{S_n}(\beta_{\max}s)$.

Proof. Increasing λ_c raises negative preemption and the frequency of slow-service state entries, while increasing β lengthens slow-state sojourns. Both operations make Y_i larger in the increasing-convex order and increase $\mathbb{E}[T_i]$. Since $\bar{\Delta}_i$ in (22) is monotone in $\mathbb{E}[T_i]$, $\mathbb{E}[Y_i]$, and $\mathbb{E}[(Y_i)^2]$, the supremum over $\mathcal{L}(\lambda_{\max}, \beta_{\max})$ is attained at $\lambda_c = \lambda_{\max}$ and $\beta = \beta_{\max}$, yielding the upper bound in (24). \square

Note that the lower bound in (23) depends only on the benign source's arrival process via H_i , thus ignoring adversarial preemptions and service slowdowns, whereas the upper bound in (24) captures the worst admissible impact of adversarial preemption and slowdowns through $(\lambda_{\max}, \beta_{\max})$.

V. NUMERICAL RESULTS AND DISCUSSIONS

In this section, we evaluate the achievable AAOI of the proposed adversarial model under Pareto (Par.), Erlang-2 (Erl.), and Hyper-exponential order-2 (Hyp.) service time distributions [7], [11]. Both numerical (Num.) evaluations and Monte Carlo (MC) simulations (averaged over 12 runs) are conducted, and the results are benchmarked against the baseline no-adversary case, i.e., $\lambda_c = 0$. For the Par. distribution, we use scale parameter $\theta = 1$ and shape $\alpha = 3$. For the Erl. distribution, we set shape $k = 2$ with rate $\mu = 4/3$, and for the Hyp. distribution, we adopt rates $(\mu_1, \mu_2) = (1, 0.5)$ (mean normalized to $1/\mu$) and

balanced mixture probability $p = 0.5$. These parameters are chosen so that the mean service time is the same across all three distributions, i.e., $\mathbb{E}[S] = 1.5$. Unless otherwise stated, we set $\lambda_{\max} = \beta_{\max} = 2$.

Fig. 3 depicts the AAOI of the benign source s_1 under three service time distributions in the two-source setting. The results show that the AAOI is highest under the Par. distribution with $\mathbb{E}[S] = \alpha\theta/(\alpha - 1)$, moderate under the Erl. distribution with $\mathbb{E}[S] = k/\mu$, and lowest under the Hyp. distribution with $\mathbb{E}[S] = p/\mu_1 + (1-p)/\mu_2$. This behavior stems from the distinct tail characteristics of the service times. The Par. distribution shown in Fig. 3a exhibits a heavy tail with a decreasing hazard rate. This implies that once a long service is encountered, it is likely to remain long. Such prolonged service times are highly susceptible to adversarial preemptions, which extend the inter-delivery intervals of the positive updates and result in higher AoI values. For Erl. service (Fig. 3b), the distribution is more concentrated around its mean with limited variability, so updates are less likely to complete unusually early and thus, leading to higher AoI relative to the Hyp. distribution shown in Fig. 3c. As for the Hyp. case, a non-negligible probability mass is concentrated at very short service durations, which substantially increases the likelihood that an update completes service before a negative arrival interrupts it, thereby reducing AoI. Hence, even under the same $\mathbb{E}[S]$, the service distribution significantly influences system timeliness, with lighter-tailed and more variable distributions favoring lower AAOI in adversarial system.

Fig. 4 compares the AAOI of s_1 versus λ_1 under the bounds derived in (23) and (24). The *lower bound* (LB), which is computed with no adversary and no slowdown ($\lambda_c = 0, \beta = 1$), decays rapidly in λ_1 because the inter-arrival shrinks as updates are generated more frequently. Hence, (23) reduces to $\mathbb{E}[S] + 1/\lambda_1$. The *upper bound* (UB), evaluated at the worst case ($\lambda_c = \lambda_{\max}, \beta = \beta_{\max}$), is the highest curve which reflects more frequent negative preemptions and slower service thus, inflating the renewal second-moment term in (24). The Num. curve ($\lambda_c = 1, \beta = 1.5$) lies between LB and UB across all λ_1 values, validating the bounding construction. Increasing the

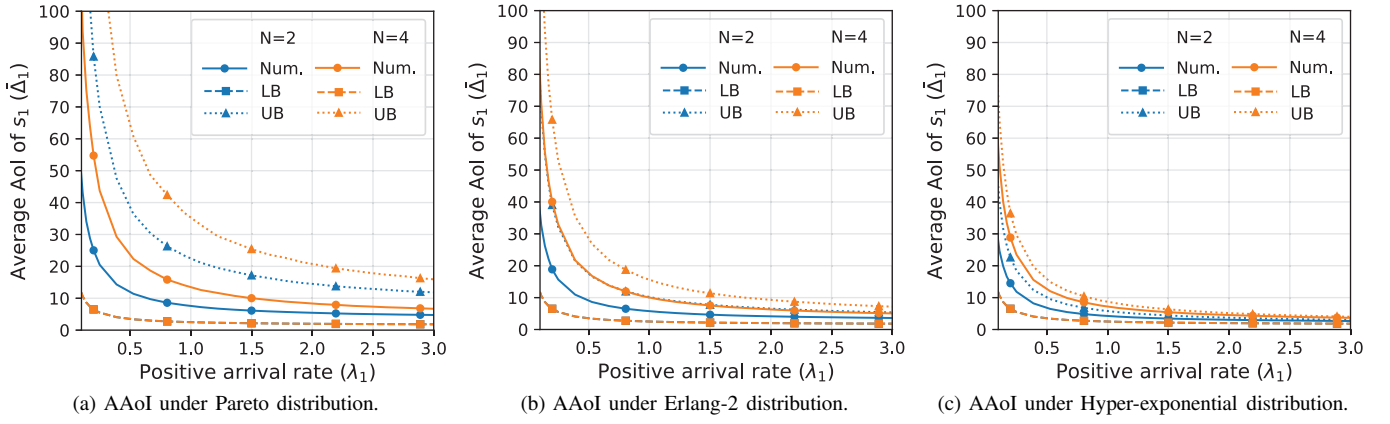


Fig. 4. AAOI bound comparisons in the M/G/1/1 system with $N \in \{2, 4\}$ sources and under different service distributions: (a) Pareto ($\theta = 1, \alpha = 3$); (b) Erlang-2 ($k = 2, \mu = 4/3$); (c) Hyper-exponential ($p = 0.5, \mu_1 = 1, \mu_2 = 0.5$). For Num., $\lambda_c = 1$ and $\beta = 1.5$.

number of sources from $N = 2$ to $N = 4$ shifts all curves upward. Evidently, extra contention raises the busy probability and the chance that status updates from s_1 are dropped or exposed to adversarial preemption, so both T_1 and Y_1 tend to grow. The heavy-tailed Par. distribution in Fig. 4a yields the largest AAOI and widest LB-UB gap because occasional very long services are highly vulnerable to preemption/slow epochs. The more concentrated Erl. distribution in Fig. 4b moderates this effect, whereas the Hyp. distribution in Fig. 4c provides the smallest AAOI since a non-trivial number of very short services often completes before a negative arrival, lowering Y_1 and in turn, the average age.

VI. CONCLUSION

In this paper, we investigated the impact of adversarial attacks on the AAOI in multi-source M/G/1/1 status updating systems. Closed-form MGFs for AoI and PAoI were derived to establish performance bounds under adversarial constraints on maximum attack rate and service slowdown. The analysis showed that the worst-case adversarial strategy yields a tractable characterization of the system's performance limits, while numerical and Monte Carlo evaluations confirmed the theoretical results and highlighted the tradeoff between adversarial intensity and service efficiency across different service distributions. Future directions include extending the model to buffer-aided queues and exploring joint optimization of energy expenditure and AoI in adversarial IoT networks.

REFERENCES

- [1] L. Chettri and R. Bera, "A comprehensive survey on Internet of Things (IoT) toward 5G wireless systems," *IEEE Internet Things J.*, vol. 7, no. 1, pp. 16–32, Jan. 2020.
- [2] M. A. Abd-Elmagid, N. Pappas, and H. S. Dhillon, "On the role of age of information in the Internet of Things," *IEEE Commun. Mag.*, vol. 57, no. 12, pp. 72–77, Dec. 2019.
- [3] R. D. Yates, Y. Sun, D. R. Brown, S. K. Kaul, E. Modiano, and S. Ulukus, "Age of information: An introduction and survey," *IEEE J. Sel. Areas Commun.*, vol. 39, no. 5, pp. 1183–1210, May 2021.
- [4] İ. Kahraman, A. Köse, M. Koca, and E. Anarim, "Age of information in Internet of Things: A survey," *IEEE Internet Things J.*, vol. 11, no. 6, pp. 9896–9914, Mar. 2024.
- [5] N. Pappas, M. A. Abd-Elmagid, B. Zhou, W. Saad, and H. S. Dhillon, *Age of Information: Foundations and Applications*. Cambridge University Press, 2023.
- [6] M. Moltafet, M. Leinonen, and M. Codreanu, "On the age of information in multi-source queueing models," *IEEE Trans. Commun.*, vol. 68, no. 8, pp. 5003–5017, Aug. 2020.
- [7] —, "Moment generating function of age of information in multisource M/G/1/1 queueing systems," *IEEE Trans. Commun.*, vol. 70, no. 10, pp. 6503–6516, Oct. 2022.
- [8] M. Moradian, A. Dadlani, A. Khonsari, and H. Tabassum, "Age-aware dynamic frame slotted ALOHA for machine-type communications," *IEEE Trans. Commun.*, vol. 72, no. 5, pp. 2639–2654, May 2024.
- [9] F. Chiariotti, O. Vikhrova, B. Soret, and P. Popovski, "Age of information in multihop connections with tributary traffic and no preemption," *IEEE Trans. Commun.*, vol. 70, no. 10, pp. 6718–6733, Oct. 2022.
- [10] A. Sinha, S. Singhvi, P. D. Mankar, and H. S. Dhillon, "Peak age of information under tandem of queues," in *Proc. of IEEE Int. Symp. Inf. Theory (ISIT)*, Jul. 2024, pp. 951–956.
- [11] M. S. Kumar, A. Dadlani, and H. Tabassum, "Age of information in unreliable tandem queues," *IEEE Commun. Lett.*, pp. 1–5, 2025, doi: 10.1109/lcomm.2025.3593785.
- [12] S. Banerjee and S. Ulukus, "Age of information in the presence of an adversary," in *Proc. of IEEE Conf. Comp. Commun. Workshops (INFOCOM WKSHPs)*, May 2022, pp. 1–8.
- [13] A. Sinha and R. Bhattacharjee, "Optimizing age-of-information in adversarial and stochastic environments," *IEEE Trans. Inf. Theory*, vol. 68, no. 10, pp. 6860–6880, Oct. 2022.
- [14] S. Banerjee and S. Ulukus, "The freshness game: Timely communications in the presence of an adversary," *IEEE/ACM Trans. Networking*, vol. 32, no. 5, pp. 4067–4084, Oct. 2024.
- [15] E. Gelenbe, "Product-form queueing networks with negative and positive customers," *J. Appl. Probab.*, vol. 28, no. 3, pp. 656–663, Sep. 1991.
- [16] J. Doncel and M. Assaad, *Optimizing Age of Information with Attacks*. Springer Nature Switzerland, 2025, pp. 3–13.
- [17] E. Najm and E. Telatar, "Status updates in a multi-stream M/G/1/1 preemptive queue," in *Proc. of IEEE Conf. Comp. Commun. Workshops (INFOCOM WKSHPs)*, Apr. 2018, pp. 124–129.
- [18] A. Soysal and S. Ulukus, "Age of information in G/G/1/1 systems: Age expressions, bounds, special cases, and optimization," *IEEE Trans. Inf. Theory*, vol. 67, no. 11, pp. 7477–7489, Nov. 2021.